

A QCD Survey: $0 \leq Q^2 \leq 10^5 \text{ GeV}^2$

Gerald C. Blazey

*Physics Department, Northern Illinois University
DeKalb, Illinois 60115-2854, U.S.A*

Selected, recent results, primarily from collider experiments but including some fixed target experiments, are presented as a survey of Quantum Chromodynamics (QCD). The concepts of leading order and next-to-leading order QCD are introduced. Inclusive $p\bar{p}$ jet and dijet production and deep inelastic ep scattering at very large momentum transfer are shown to be in good agreement with perturbative QCD (pQCD). Dijet, three-jet and multi-jet results from $p\bar{p}$, ep , and ee colliders at moderate Q^2 are also compared to pQCD. BFKL searches from all three colliders are discussed. Recent measurements of structure functions and contributions to the parton distribution functions are presented. New measurements of α_s are summarized, the world average is $\alpha_s = 0.1184 \pm 0.0031$.

1. Introduction and a Brief Introduction to QCD

Quantum chromodynamics (QCD) beautifully describes the strong interaction over a surprisingly broad range of phenomena - from the non-perturbative regime of hadronic structure to the highest energies observed in particle colliders. Recent measurements of high momentum transfer jet production and deep inelastic scattering, multi-jet production, proton parton distribution functions, and the strong coupling constant convincingly illustrate the breath of experimental progress. These results have, in turn, stimulated impressive theoretical progress and sensitive searches for new interactions and dynamics. Because of the immense quantity of QCD research underway the results discussed here are necessarily and unfortunately incomplete, this document might best be viewed as an introductory overview.

The proton-antiproton interaction, a general scattering process, nicely introduces the concepts of leading order and next-to-leading order perturbative quantum chromodynamics. Inelastic scattering between a proton and an antiproton can be described as an elastic collision between a single proton constituent and single antiproton constituent. These constituents are collectively referred to as partons and in QCD are quarks and gluons. Predictions for jet production are given by folding experimentally determined parton distribution functions f with quark and gluon two-body scattering cross sections $\hat{\sigma}$. The two ingredients can be formally combined to calculate any cross section of interest: $\sigma = \sum_{i,j} \int dx_1 dx_2 f_i(x_1, \mu_F^2) f_j(x_2, \mu_F^2) \sigma[x_1 P, x_2 P, \alpha_s(\mu_R^2), Q^2/\mu_F^2, Q^2/\mu_R^2]$. The nonperturbative parton distribution function $f_k(x_l, \mu_F^2)$ describes the momentum fraction x of the beam momentum P carried by the l^{th} parton of type k . The hard two-body interaction between the gluon and quark partons can be calculated with perturbative QCD (pQCD) and is a function of the perturbative or strong coupling constant α_s , the hard scale momentum

transfer between incoming particles Q , and the renormalization scale μ_R .

The factorized scattering has been illustrated with a leading order (LO) process; that is, a process with the minimum number of vertices (or coupling constants) to describe two final states. Although useful, the leading order picture (where one parton results in one jet) is too simple and has an unphysical dependence on μ_R . Next-to-leading order (NLO), or for this two jet process $O(\alpha_s^3)$ calculations, include additional parton emission and have reduced sensitivity to μ_R . Depending on the proximity of the outgoing partons, a “jet” could result from one or the combination of two partons. NLO calculations crudely model fragmentation, thereby obviating the need for fragmentation functions.

2. QCD at the Highest Momentum Transfers

A complete theoretical description of inclusive jet production, $p\bar{p} \rightarrow j + X$, requires proper treatment of the final state radiation and accurate measurements of the parton distribution functions, pdf’s. The inclusive jet cross section is reported as $d^2\eta/dE_T d\eta$. $E_T = E \sin\theta$ where E is jet energy and θ the angle between the proton direction and the jet. The pseudorapidity, η , is defined as $-\ln(\tan(\theta/2))$. Kinematically, an individual jet is characterized by E_T , η , and azimuth ϕ . Jets are found by clustering energy in a cone of radius 0.7 in $\eta - \phi$ space ¹.

The inclusive jet cross section has been intensively studied at beam energies of 900 GeV/c at the Fermilab Tevatron proton-antiproton collider in Batavia, Illinois by the DØ collaboration for $|\eta| < 3.0$ ^{2,3} and by the CDF collaboration in the region $0.1 < |\eta| < 0.7$ ^{2,4}. The data now span nearly ten orders of magnitude for jet energies between 20 and 450 GeV. The percentage difference as a function of E_T between the data and theory normalized to the theory for the DØ data is shown in Fig. 1. Events at the highest E_T correspond to x values of 0.5 and Q^2 greater than

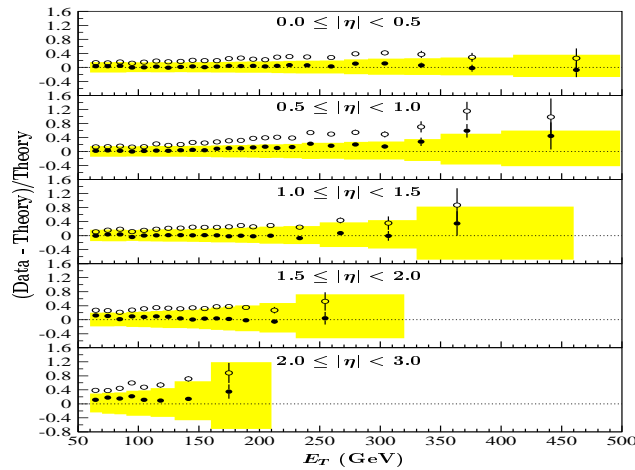


Figure 1: The difference between the inclusive cross section and NLO theory normalized to NLO theory.

10^5 GeV^2 . Data points include statistical errors only and the bands indicate the magnitude of the systematic errors. The figure includes a NLO prediction ⁵ using the CTEQ4HJ pdf. There is excellent agreement at all E_T and η and, in particular, no indication of excess production at large E_T . The CDF collaboration finds similar agreement in the region $0.1 < |\eta| < 0.7$, but reports a 25% discrepancy ² for E_T above 400 GeV.

The good agreement is in sharp contrast to an earlier, lower statistics results from the CDF collaboration which suggested excess production at large E_T relative to contemporaneous NLO predictions ⁴. The early CDF results prompted a closer look at theoretical and pdf uncertainties contributing to the predictions. In fact, inspired by the initial CDF result, the CTEQ4HJ pdf used in Fig. 1 includes a strengthened high-x gluon component. All DØ and CDF results are consistent within statistical and systematic errors ⁶.

The dijet mass distribution for the leading two jets of a $p\bar{p} \rightarrow j + j + X$ event at beam energies of 900 GeV also constitutes a sensitive search for new physics. The cross section is reported as $d^3\eta/dM_{jj}d\eta_1d\eta_2$ where M_{jj} is the invariant mass of the leading two jets. Both DØ and CDF have published results which show good agreement between data and NLO QCD ^{7,8,9}. As shown in Fig. 2, the DØ collaboration has taken the ratio of the central dijet mass distribution $|\eta| \leq 0.5$ to the forward distribution, $0.5 \leq |\eta| \leq 1.0$. This distribution is sensitive to quark compositeness because the associated jet production will be predominantly central in rapidity. In a manner completely analogous to Rutherford scattering, excess jet production at very large transverse energies signals the presence of quark compositeness. The curves in Fig. 2 include NLO predictions with and without a additional jet production due to compositeness. The solid curve postulates no substructure, and DØ has set a limit of 2.4 TeV or $\sim 10^{-19}$ m on any substructure ⁸.

HERA, an electron-proton collider in Hamburg, Germany provides a complementary and comprehensive opportunity to examine QCD over a very large range of momentum transfer (0 to $3 \times 10^4 \text{ GeV}^2$). The introductory description of $p\bar{p}$ jet

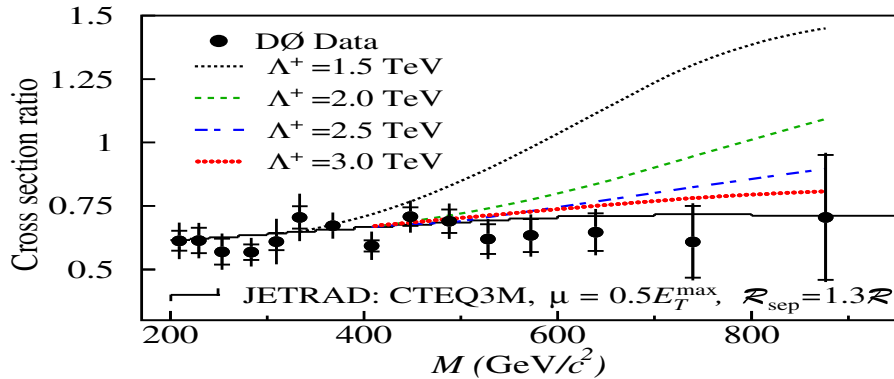


Figure 2: Comparisons of central to forward dijet cross section ratios as a function of mass to theoretical predictions. See text for details.

production can be modified to ep scattering if one incoming hadron is replaced with an electron and the exchanged gluon by an electroweak boson. A neutral current (NC) reaction is characterized by an exchanged photon or Z , while charged current (CC) reactions involve an exchanged W . The CC and NC cross sections are reported as $d^2\sigma/dQ^2$. HERA ran from 1994–1997 with positrons at a center-of-mass energy of 300 GeV and from 1997–1998 with electrons at an energy of 320 GeV.

As shown in Fig. 3, the $ep \rightarrow e + X$ neutral current cross section spans eight orders of magnitude¹⁰. Below $Q^2 = 10^4 \text{ GeV}^2$ the data are well described by NLO theory. However, the NC e^+p data shows excess production at very high Q^2 , an effect observed (and which generated great excitement) by both the H1 and ZEUS collaborations in the 1994–1997 data set^{11,12}. In contrast, the 1997–1998 e^-p NC cross section (also shown in Fig. 3) and similar results from the ZEUS collaboration¹³ are both well described within statistical errors at all Q^2 by NLO QCD. Although not shown, CC $ep \rightarrow \nu + X$ cross sections for both electrons and positrons are also well described by QCD^{10,13}.

The $p\bar{p}$ and ep colliders both test the limits of QCD and the Standard Model (SM) at the highest momentum transfer. In the mid-nineties hints of excess jet and NC events at large E_T or, equivalently, Q^2 were observed at both colliders. However, since then new results (characterized by higher statistics or new projectiles) and modified theoretical predictions (characterized by new pdfs), strongly suggest the SM can currently describe the data. The lure of new physics is exciting and searches for high Q^2 discrepancies will continue, especially with the ever increasing statistics at HERA and Fermilab. However, as seen in the next section, the lower Q^2 regime of multi-jet production proves an interesting window onto the behaviour of QCD.

3. Multijet Production

All three colliders, HERA, the Tevatron, and the LEP e^+e^- machine in Geneva, Switzerland prove prolific laboratories for the study of multi-jet production. At HERA and LEP jets are conventionally found with recombination algorithms which cluster energy according to their proximity in E_T , η , and azimuth¹. At LO, HERA dijet production occurs through the QCD Compton graph (where a photon from the incoming lepton scatters off a quark from the hadron to produce a gluon jet and quark jet) and through the boson-gluon fusion graph (where a gluon from the hadron splits into a $q\bar{q}$ pair, one of which scatters off a photon from the incoming lepton, to produce a quark and antiquark jet). The $\sim 100 < Q^2 < \sim 10^4 \text{ GeV}$, rapidity, mass, and x distributions of these dijet cross sections are generally well described by NLO QCD¹⁴.

The NLO dijet predictions, which include up to three emitted partons, represent LO predictions for three jet production. These LO, three jet predictions are in reasonable agreement with HERA three jet cross sections as a function of Q^2 and M_{3jet} ¹⁵. There does seem to be a discrepancy between data and theory for the ratio of three to two jet cross sections. At Q^2 below 1000 GeV^2 the experimental ratio is below the LO prediction¹⁵. However, parton shower simulations show excellent

agreement with the data, this is typically a signal that higher order perturbative QCD predictions will show improved agreement. The ratio of three jet to two jet cross sections has also been measured at the Tevatron as a function of the sum of the E_T of all jets in the event ΣE_T ¹⁶. The ratio rises rapidly with ΣE_T but levels off at 0.7 above 200 GeV. The data is fairly well described by LO QCD, but as expected is sensitive to the choice of renormalization scale.

Recently a theoretical milestone was reached with the completion of NLO three jet predictions¹⁷. At NLO three jet predictions includes three and four parton final states. Figure 4 shows a Dalitz lego plot calculated with NLO QCD, where $x_i = 2E_i/M_{3,J}$ and the indices $i = 3, 4, 5$ represent the final state jets ordered in energy, E_i is the energy of the three jets, and $M_{3,J}$ the invariant mass of the jets. The pronounced peaking a $x_4 = x_3 \sim 1$ indicates that the third jet is of low energy or that the events are primarily two jet in nature. The CDF collaboration has made preliminary measurements of the Dalitz distributions and reports good agreement, however uncertainty analysis are pending¹⁸.

Multijet production also offers an opportunity to search for new dynamics. Al-

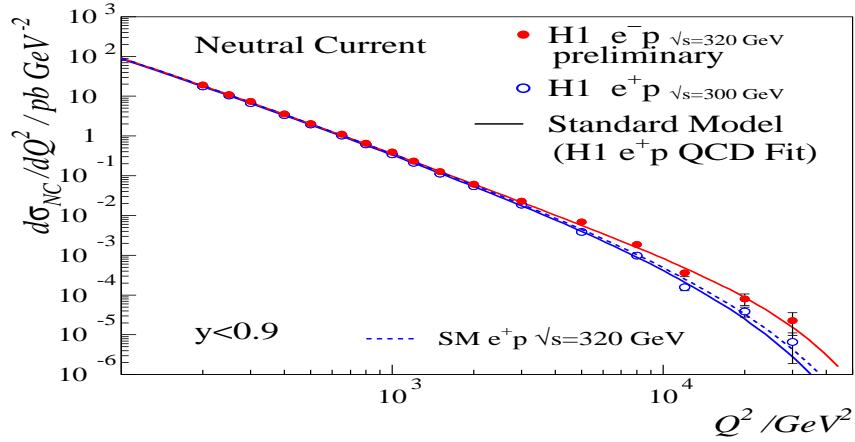


Figure 3: Neutral current cross sections for e^+p and e^-p scattering compared to Standard Model expectations.

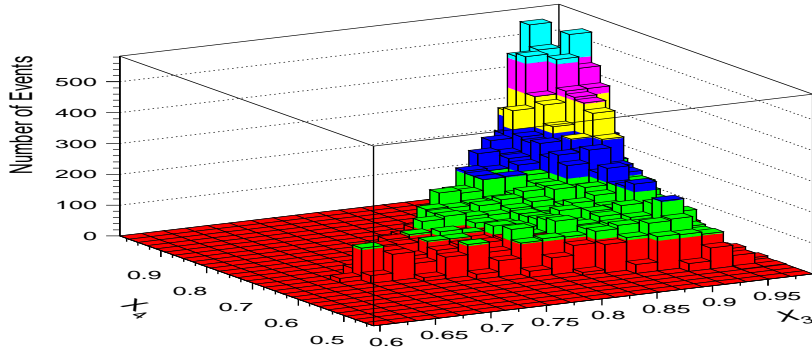


Figure 4: A Dalitz plot of a NLO three jet cross section.

most all QCD data are well described by DGLAP evolution which can be characterized by partonic emission strongly ordered in Q^2 . The familiar expansion $\sigma \sim (\alpha_s \ln Q^2)^n$ describes a remarkable range of x and Q^2 . (See the discussion of Structure Functions, for example.) However, at fixed Q^2 and small x , Balitsky-Fadin-Kuraev-Lipatov or BFKL evolution may be appropriate¹⁹. Here $1/x$ becomes large and cross sections are of the form $\sigma \sim (\alpha_s \ln(1/x))^n$ where $x = Q^2/s$ and s is the center-of-mass energy. Terms in $\alpha_s \ln(1/x)$ correspond to gluon emission strongly ordered in x .

At the Tevatron, for events characterized by two jets widely separated in $\Delta\eta$, the term $\alpha_s \ln(1/x)$ is proportional to $\alpha_s \Delta\eta$. BFKL resummation²⁰ of these leading log terms yields an exponential increase of σ with $\Delta\eta$, $\sigma \sim e^{\Delta\eta}$, this approximation is valid only for $\Delta\eta > 2$. Crudely, a gluon ladder between the outgoing partons increases the cross section. However, the exponential growth is moderated by momentum conservation (equivalently the pdf's). Sensitivity to the exponential increase can be found in the ratio of cross sections at different center-of-mass energies but identical x_1 and x_2 so that the pdf damping cancels. This ratio has been measured at Tevatron energies²¹ of 1800 and 630 GeV. The data for $\Delta\eta > 2$ is well above and inconsistent with exact LO and HERWIG predictions. (Herwig is a LO simulation which includes fragmentation and hadronization). The BFKL prediction best describes the data but is also 3σ below the observation.

HERA is a natural site for BFKL searches since x values near 10^{-5} are accessible. For example, inclusive π^0 production for $10^{-4} < x < 10^{-2}$ and $2 < Q^2 < 70 \text{ GeV}^2$ is well described by LO BFKL predictions but poorly described by LO QCD²². Likewise forward jet production or production in the beam direction, $1.5 < \eta < 2.8$ and $10^{-4} < x < 10^{-2}$ is not described by NLO QCD²³. There is also a pronounced dependency on the choice of renormalization scale. This suggests that the calculations are incomplete and something more is needed, perhaps BFKL improvements, a better description of the photon structure function, or next-to-next-to-leading order terms.

BFKL dynamics are also accessible at LEP through $\gamma^* \gamma^*$ scattering where each incoming lepton radiates a virtual photon. At LO the photons scattering off a $q\bar{q}$ pair. At higher orders each photon emits a $q\bar{q}$ pair and the two pairs interact through gluon exchange. The L3 experiment at LEP has measured a rise in $\sigma(\gamma^* \gamma^*)$ as a function of the scattering center-of-mass²⁴. This increased cross section can be attributed to the the phase space opened up by emission of additional gluons from the exchanged gluon. The rise is not described by LO QCD but is described by a BFKL prediction. There are abundant hints for the existence of BFKL dynamics; however, all searches need improved higher-order calculations, both DGLAP and BFKL, before the origins of these hints are clear. Moreover, DGLAP has been impressively successful over almost all x and Q^2 .

4. The Structure of the Proton

The proton pdf's are derived from global fits to two general types of data: structure

functions from e , μ and ν scattering from nuclear targets and from exclusive state production such as Drell–Yan, charm, W, jet, and photon production. Without going into details, trial pdf’s are evolved from a starting Q_o , convoluted with QCD calculations of the hard scatter, and fit to the observed data. These pdf’s are assumed to be universal in that a single unique pdf is appropriate for all reactions. Each reaction does, however, provide access to a particular type of pdf. For instance, W production in $p\bar{p}$ scattering directly accesses the u and d quark pdfs. Generally, quark functions are heavily constrained by DIS scattering for $x < 0.9$. Until recently there has been very little to constrain gluons ²⁵ above $x > 0.2$ (This freedom permitted the formulation of pdf’s similar to CTEQ4HJ used in Fig. 1.) Recent developments in pdf derivations include an increased accuracy due to new types of input data, replacement of prompt photon data with jet data, and concerted efforts to improve the treatment of uncertainties. For a summary consult the references ²⁶.

The differential cross section $d^2\sigma^{NC}/dx dQ^2$ for NC scattering, where x is the momentum fraction of the struck quark, can be expressed at leading order in terms of the structure functions $F_2(x, Q^2)$ and $F_3(x, Q^2)$. F_2 is proportional to the sum of the valence and sea quark pdf’s, $q(x, Q^2) + \bar{q}(x, Q^2)$. F_3 is proportional to the difference of the valence and sea quark pdf’s, $q - \bar{q}$. Figure 5 shows F_2 for $0.000032 < x < 0.65$ and $1 < Q^2 < \sim 10^4 \text{ GeV}^2$ as measured by the H1, SLAC, NMC and BCDMS

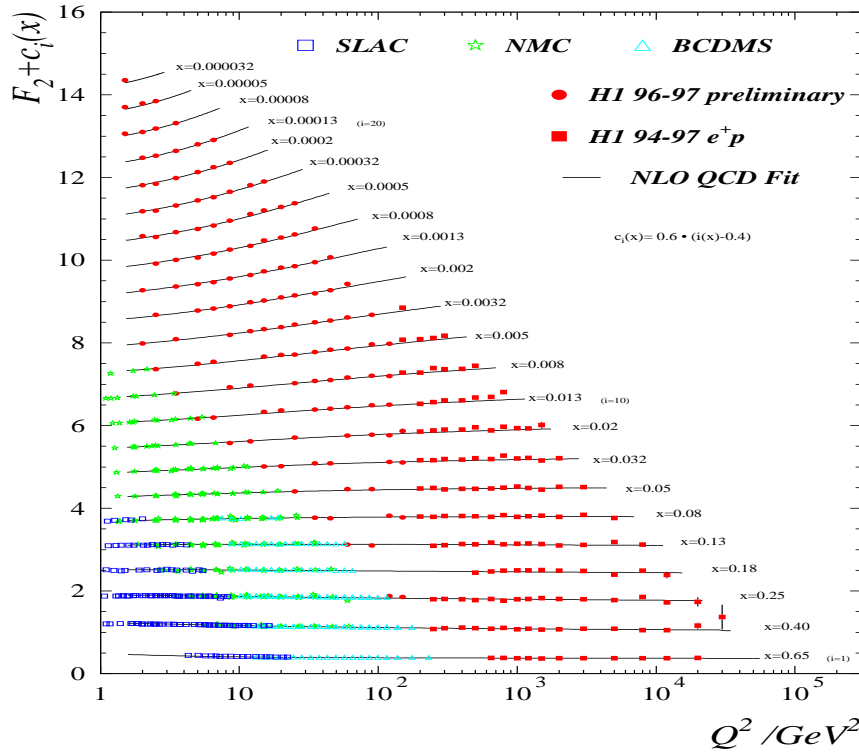


Figure 5: A compilation of structure functions over a wide range of x and Q^2 .

collaborations. (To aid the eye the data at each value of x is offset by an arbitrary constant.) The H1 data is recent, and ZEUS has made similar measurements ²⁷. The curves correspond to a NLO QCD fit and include both e^+p and e^-p data. The astonishing agreement includes both the large Q^2 perturbative region and also the small, presumably, nonperturbative Q^2 regions. The dependence of F_2 on Q^2 at low- x region is an example of QCD scaling violations. Although not shown, the availability of both e^+p and e^-p NC data also permits measurement of F_3 , these results are in agreement with NLO QCD ²⁸.

Charge current reactions couple directly to the quark distributions. Specifically, $d^2\sigma^{CC}(e^-p)/dx dQ^2$ is proportional to the u and c quark distributions, and $d^2\sigma^{CC}(e^+p)/dx dQ^2$ is proportional to the d quark. Figure 6 shows a reduced CC cross section for various Q^2 bins as a function of x for e^-p data ²⁹. The uppermost curve in each panel represents the total cross section as predicted by NLO QCD using the CTEQ5D pdf. Agreement is good at all x and Q . The lower curves indicate the contribution from each type of quark. As expected the u quark contribution is dominant.

Additional constraints on the quark distributions below $x \sim 0.7$ can be derived from fixed target and $p\bar{p}$ scattering. A few recent examples are listed here. The CCFR collaboration has re-analyzed its ν and $\bar{\nu}$ DIS data and finds F_2 for $0.015 < x < 0.175$ and $1 < Q^2 < 100 \text{ GeV}^2$ well described by updated NLO QCD

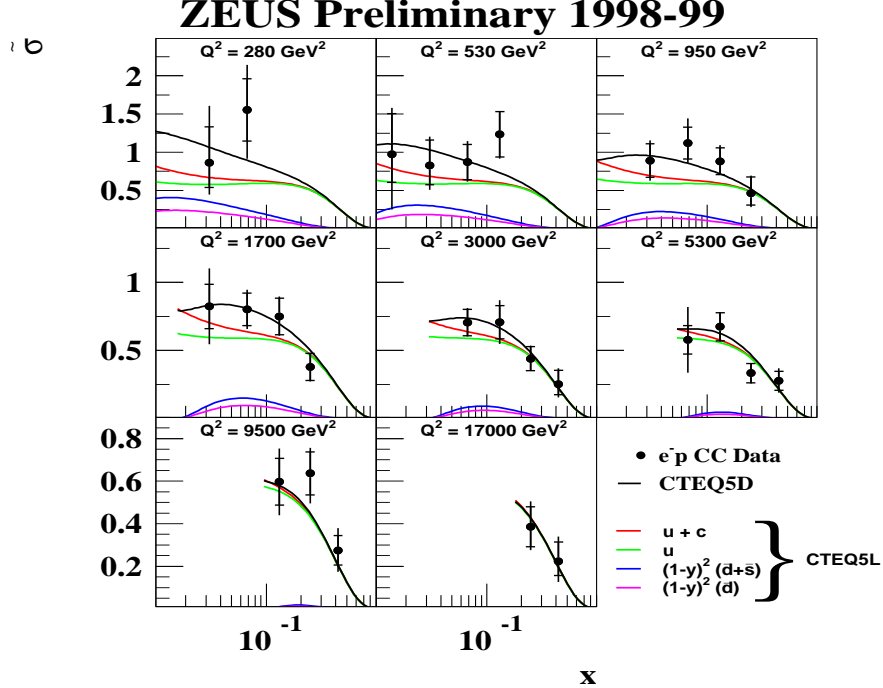


Figure 6: The CC cross-section at various x and Q^2 with predictions for the various quark contributions.

predictions³⁰. CCFR has also made the first measurement of $F_3^\nu - F_3^{\bar{\nu}}$. The rapidity distributions of the final state leptons in the Drell–Yan process $p\bar{p} \rightarrow \gamma^*/Z \rightarrow e^+e^-$ is sensitive to the valence quark distributions. For example, if the two initial partons are of unequal momentum the virtual γ^*/Z will be boosted in the direction of the more energetic parton and the decay electrons will likewise be boosted. Analysis of the rapidity distributions as recently measured by the CDF collaboration constrains the u and d distributions for $0.05 < x < 0.6$ ³¹. Recent results also pertain to the sea-quark distributions, the cross sections for $\mu^+\mu^-$ production from pp and pd scattering as measured by the E866 collaboration constrains the $\bar{d} - \bar{u}$ sea distribution between $x \sim 0.03$ and ~ 0.3 ²⁶.

As mentioned earlier, the large- x gluon distributions are not well known. Until recently, a favored process for constraining $g(x)$ in the global fits was direct photon production. The associated Compton graph samples $g(x)$ directly. However, this process has fallen out of favor since NLO calculations cannot describe the world data³². For nearly every photon cross section measurement, the data exceeds theory at the low end of that specific measurement's x range. This discrepancy has been attributed to initial-state soft radiation which manifests itself as transverse momentum or k_T . If not interpreted correctly, this k_T or "kick" adds to the measured x of the photon which creates the observed excess of data over theory. Evidence for k_T comes from events where object pairs such as pions, diphotons, dimuons, and dijets are produced. The vector sum of the pair momentum is a direct measure of the parton scatter transverse kick. Indirect evidence comes from the observation that augmentation of NLO predictions with a phenomenological addition of k_T dramatically improves agreement between data and theory. Also, the importance of soft gluon resummation for Drell–Yan, diphoton, W, and Z production was recognized some time ago. Similar calculations for direct photon production are underway and already show much better agreement between data and theory. Perhaps with time and higher orders photon data will return to the pdf fits.

In the meantime, the central inclusive jet cross sections constrain $g(x)$ for $\sim 0.05 < x < \sim 0.5$. Inclusion of the full inclusive cross section for $p\bar{p}$ scattering over $|\eta| < 3.0$ will cover $x < \sim 0.8$ ². Even more can be gained from triple differential cross sections, $d^3\sigma/dE_T d\eta_1 d\eta_2$ where E_T corresponds to the leading jet in an event and the subscripts identify the leading two jets⁶. For a dijet event if both jets are at $\eta = 0$ with $E_T = 180 \text{ GeV}$ then $x_1 = x_2 = 0.2$. However, for $\eta = 0$ and $E_T = 90 \text{ GeV}$ with the second jet at $\eta = 2$, $x_1 = 0.2$ and $x_2 = \sim 0.9$. Since the event structure is boosted forward a much greater fraction of the initial hadron momentum is required. Both Tevatron experiments are encouraged to publish their preliminary differential cross sections^{6,18} since NLO predictions exist and the data could be incorporated into the pdf's. Dijet production at HERA, through the boson fusion graph, also directly measures $g(x) < 0.1$ ³³. Although the data doesn't greatly alter the pdfs's relative to the F_2 data it does add stability to the fits and reduce errors.

Until recently the uncertainties of observables due to pdf's were estimated merely by using a menu of pdf's. However, pdf's should more properly handle statistical

and systematic data uncertainties, theoretical uncertainties, and parameterizations. In the past year or two, there has been very great progress dealing with these uncertainties^{34,35,36}. For instance, the plot below by Botje shows the allowed variations in the gluon and quark distributions due to statistical uncertainties, input choices, analysis cuts, and renormalization choices assuming all uncertainties are symmetric and Gaussian in nature³⁴. Notice the unconstrained nature of the gluon distributions, Tevatron jet results were not included in this calculation. An even more general approach by Giele and Keller incorporates probability distributions to derive the pdf's³⁵. These authors and others are providing tools for incorporating all sources of pdf uncertainties.

5. Status of α_s Measurements

An enormous body of research has been dedicated to the study of the strong coupling constant, α_s since it is the only free parameter of QCD and must be determined experimentally. Of equal interest is the dependence of the coupling constant on momentum transfer Q^2 , $\alpha_s(Q^2) = 12\pi/(33-n_f)\log(Q^2/\Lambda^2)$ where n_f is the number of quark flavors and Λ is experimentally determined. Notice α_s decreases or “runs” with momentum transfer. This is, in fact, the basis for the perturbative NLO QCD calculations described earlier.

The strong coupling constant can be derived in a myriad of ways and at all Q^2 , from absolute decay rates of the Z boson and τ lepton, energy levels of bound heavy quarks, jet event shapes, jet production rates and angular distributions, and scaling

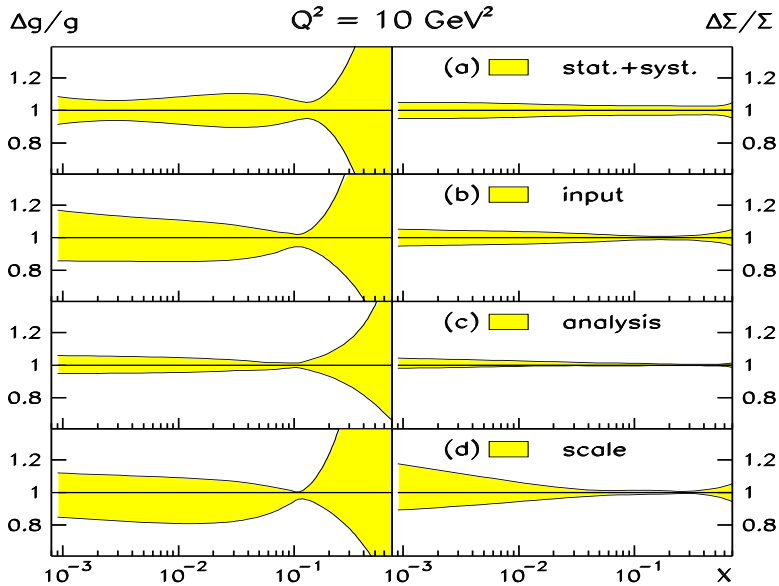


Figure 7: Allowed variations of the gluon and quark pdf's assuming symmetric Gaussian uncertainties associated with the global fit.

violations in deep inelastic scattering. Notable new measurements of α_s originate from all three high energy colliders. In particular, the LEP collaborations recently ran at center-of-mass energies from 192 to 202 GeV and from event shape and jet rate measurements determined an average $\alpha_s(198\text{GeV}) = 0.109 \pm 0.001 \pm 0.005$ where the first error is statistical and the second theoretical³⁷. A uniform re-analysis of e^+e^- event shapes, jet rates, and multiplicities from the JADE and LEP collaborations from center-of-mass energies between 20 and 200 GeV show the strong coupling constant obviously running with a value of $\alpha_s(M_Z) = 0.1208 \pm 0.0006 \pm 0.0048$ ³⁷. Finally, comparison of NLO inclusive jet and dijet cross section predictions to experimental results from HERA and the Tevatron consistently yield $\alpha_s(M_Z)$ measurements near 0.12^{33,38}. The Tevatron inclusive jet measurement beautifully demonstrates the running of α_s over $10^3 < Q^2 < 2 \times 10^5 \text{ GeV}^2$.

An excellent review by Bethke includes a comprehensive compilation of the many derivations of α_s complete with a description and evaluation of each measurement³⁹. The current world average for the coupling constant, $\alpha_s(M_Z) = 0.1184 \pm 0.0031$, is based on six measurements for which next-to-next-to-leading order predictions exist. The average is known to better than 3% and is unchanged since 1997⁴⁰.

6. Conclusions

QCD, and in particular perturbative QCD, describes the strong interaction over an impressive kinematic range. At the highest Q^2 accessible, recent data and analyses reveal few, if any, excursions from the Standard Model. At intermediate Q^2 , jet and multi-jet studies have permitted a closer study of higher order process and searches for BFKL dynamics. These searches are ambiguous. The proton structure functions are under intense study. Although the quark components are well constrained, the gluon component is not well measured for $x > 0.2$. Recent jet and, if rehabilitated, photon production data should improve this situation. There has also been great progress on pdf error analysis. Data from all values of Q^2 have contributed to a precise 3% measurement of the strong coupling constant.

Acknowledgements

Many individuals from the Tevatron, HERA, LEP and fixed target experiments have assisted with the preparation of this document. Space does not permit individual recognition, many thanks to all. I would also like to acknowledge the support of the NSF.

References

1. G.C. Blazey *et al.*, “Run II Jet Physics”, hep-ex/0005012, (2000).
2. L.Babukhadia, “Central and Forward Inc. Jets at the Tevatron”, hep-ex/005026, (2000).
3. B. Abbott *et al.*(DØ), Phys.Rev.Lett. **82** 2451 (1999).
4. F.Abe *et al.* (CDF), Phys. Rev. Lett., **77** 438 (1996).
5. W.T.Giele, E.W.N.Glover, and D.A.Kosower, Nucl. Phys. B**403**, 633 (1993) and S.Ellis *et al.* Phys. Rev. Lett., **64** 2121 (1990).

6. G.C.Blazey and B.L.Flaugher, *Ann.Rev.Nucl.Part.Sci.*, **49** 663 (1999).
7. B. Abbott *et al.* (DØ), *Phys.Rev.Lett.*, **80** 666 (1998) and F.Abe *et al.* (CDF), *Phys. Rev. Lett.*, **77** 5336(1996).
8. B. Abbott *et al.* (DØ), *Phys.Rev.Lett.*, **82** 2457 (1999).
9. F.Abe *et al.* (CDF), *Phys. Rev.*, **D48** 998 (1993).
10. K.Nagano (H1), “Inclusive Measurement of DIS Scattering at High Q^2 in e^+p Collisions at HERA”, ICHEP2000, Osaka ,Japan (2000).
11. J. Breitwig *et al.* (ZEUS), *Eur.Phys.J* **C11** 427 (1999).
12. C. Adloff *et al.* (H1), *Eur. Phys.J.* **C13** 609 (2000).
13. (ZEUS), “Measurement of high- Q^2 CC cross sections in e^-p DIS at HERA” and “Measurement of high- Q^2 NC cross sections in e^-p DIS and a first measurement of the structure function xF_3 at HERA”, ICHEP2000, Osaka Japan.
14. C. Adloff *et al.* (H1), hep-ex/0010054 (2000) and (ZEUS), “Inclusive jet cross sections in NC DIS in the Breit Frame” and “Measurement of differential cross sections for dijet production NC DIS at high Q^2 and determination of α_s ”, ICHEP2000, Osaka Japan.
15. (H1), “Study of Three-Jet Production in DIS $e+p$ Collisions at HERA” HEP99, Tapere Finland, H1prelim-99-141, (2000).
16. B. Abbott *et al.* (DØ), *Sub.Phys.Rev.Lett.*, hep-ex/0009012 (2000).
17. W.Kilgore and W.Giele, “Hadronic 3-Jet Production at NLO”, hep-ph/9903361 (1999).
18. A.Brandel, “NLO 3-jet Comparisons at the Tev.”, Moriond QCD, LesArcs,France (2000).
19. Y.Y. Balitsky and L.N. Lipatov, *Sov. J. Nucl. Phys.* **28**, 822 (1978).
20. A.H. Mueller and H. Navelet, *Nucl. Phys.* **B282** 727 (1987).
21. B. Abbott *et al.* (DØ), *Phys.Rev.Lett.*, **84** 5722 (2000).
22. C. Adloff *et al.*, (H1), *Phys. Lett.* **B462** 440 (1999)
23. T. Schoerner, (H1) “Single-inclusive and Forward Jets at low Q^2 at HERA”, ICHEP2000, Osaka, Japan, H1prelim-00-032, (2000).
24. C.Lin, “Meas. of $\gamma^*\gamma^*$ collisions at LEP”, Moriond QCD, Les Arcs, France (2000)
25. S.Kuhlmann *et al.*, “Parton Densities at High-x”, hep-ph/0007141, (2000).
26. U.Bassler *et al.*, “Sum. of the SF Work. Group at DIS99”, hep-ex/9906027, (1999).
27. E.Rizvi (H1), “NC and CC DIS at High Q^2 ” and A.Kappes (ZEUS), “NC/CC DIS at very high Q^2 ”, DIS2000, Liverpool, UK (2000).
28. N.Tuning, “Proton SFs F2 and xF3 at ZEUS”, DIS2000 Liverpool, UK, (2000).
29. (ZEUS), “Measurement of high- Q^2 CC cross sections in e^-p DIS at HERA”, ICHEP2000, Osaka, Japan (2000).
30. A. Bodek, these proceedings and hep-ex/0009061, (2000).
31. T.Affolder *et al.* (CDF) *Sub.Phys. Rev.Lett.*, hep-ex/0006025, (2000).
32. L.Apanasevich *et al.*, “Examination of direct-photon and pion production in proton-nucleon collisions”, hep-ph/0007191, (2000).
33. T. Hadig, “The strong coupling and the gluon density from jets in DIS”, DIS Workshop, Liverpool, hep-ex/0008027 (2000).
34. M.Botje, “A QCD Analysis of HERA and Fixed Target Structure Function Data”, hep-ph/9912439, (2000).
35. W.Giele, private communication, (2000).
36. L.deBarbaro *et al.*, Parton Distributions Working Group: QCD and Weak Boson Physics at Run II Workshop, Fermilab, Batavia, IL (2000).
37. O.Biebel, “ α_s : Evolution from 35 Gev to 202 Gev and flavour independence”, Moriond QCD, Les Arcs, France (2000)
38. W.T.Giele, E.W.N.Glover, J.Yu, *Phys. Rev.* **D53**, 120 (1996) and www-cdf.fnal.gov
39. S.Bethke, *J. Physics G*, **26** 27 (2000).
40. M.Schmelling, “Status of the Strong Coupling Constant”, ICHEP, Warsaw, (1996).